A millimeter and sub-millimeter wave frequency selective surface beamsplitter for geostationary orbit microwave radiometers

Cui Guang-Bin(崔广斌)†, Zhao Hai-Bo(赵海博), Zhang Yong-Fang(张勇芳), and Miao Jun-Gang(苗俊刚)

Microwave Engineering Laboratory, Beihang University, Beijing 100191, *China*

(Received 21 May 2012; revised manuscript received 1 July 2012)

We report the design of three frequency selective surface (FSS) filters used on the FengYun-4 (FY-4) microwave satellite, which separate five-frequency bands in the frequency range of 50–429 GHz with the insertion loss less than 0.4 dB, and separation between adjacent channels more than 20 dB for either TE or TM incidence. Firstly, we briefly introduce the disadvantages of two types of FSS filter: waveguide-array FSS and printed FSS, which are commonly employed in the millimeter and sub-millimeter wave band. In order to meet the insertion loss requirement and specified spectral transmission response, we adopt a filter composed of two closely spaced freestanding metal plates, which contains an array of resonant ring slot elements. Computer simulation technology (CST) is used to optimize the structural dimensions of the resonant unit and interlayer separation. Numerical results show that these FSS filters exhibit transmission loss of less than 0.4 dB and separation between adjacent channels of more than 20 dB. Simulated transmission coefficients are in close agreement with the required specification, and even exceed the performance specifications.

Keywords: millimeter and sub-millimeter wave, frequency selective surface, quasi-optical system

PACS: 41.20.–q, 41.20.Jb, 42.15.Eq **DOI:** 10.1088/1674-1056/21/11/114101

1. Introduction

With the demand of geostationary orbit observation, and recent advances in quasi-optical system and millimeter/sub-millimeter wave technology, much attention has been attracted in developing millimeter and sub-millimeter wave radiometers for remote sensing applications.[1] Such instruments often have multiple sounding bands over a wide frequency spectrum, in which case the insertion loss of traditional guided wave structures has become unacceptable. The metal waveguide loss increases with frequency, and the loss of these single-mode transmission systems become unsuitable for general system use at millimeter and sub-millimeter spectrums. To reduce loss, quasi-optical systems are introduced, which take advantage of the essentially lossless nature of the propagation of electromagnetic radiation in free space. The quasi-optical solution is able to deal with multiple polarization and operate over a very large bandwidth. In this solution, the incoming signal is demultiplexed using one or more frequency selective surfaces (FSS) and then transports the signals quasi-optically through a chain of mirrors or lenses to the feed horn and receiver for each of the bands of interest.

The FengYun-4 (FY-4) microwave satellite is China's next generation geostationary orbit meteorological satellite and is currently being developed. The microwave radiometer on the FY-4 microwave satellite is able to acquire all-time and all-weather atmospheric parameters, such as temperature profiles, humidity profiles, cloud liquid water, etc, which are crucial in weather forecasting and climate research. The sounding frequency of the microwave radiometer spans from millimeter wave to sub-millimeter wave, including a total of five frequencies bands: 54 GHz, 118 GHz, 183 GHz, 380 GHz, and 425 GHz, respectively. To satisfy satellite payload constraints on cost, mass, and energy consumption, the FY-4 antenna system employs a mechanically scanning real aperture reflector antenna, whose diameter is about 3 meters. The antenna has two reflectors, a parabolic main reflector, and a hyperboloid sub-reflector, as shown in Fig. 1(a). The quasi-optical multiplexer is a critical subsystem in the antenna system. The multiplexer separates the signal outputting from the sub-reflector

†Corresponding author. E-mail: cgbsdlg@126.com

© 2012 Chinese Physical Society and IOP Publishing Ltd

into five frequency bands, and then transmits the signal beams to the respective receiver. Additionally, the multiplexer is able to provide a proper antenna illumination pattern in order to satisfy the requirements of spatial resolution and high main beam efficiency (typically $> 90\%$) of the antenna.

The electrical requirements of the FY-4 five-frequency-band quasi-optical multiplexer are shown in Table 1. The insertion loss for each frequency band is less than 0.8 dB, and the 15-dB half-beam width of output beam for the quasi-optical multiplexer is $4.3 \pm 0.1°$. Within the instrument, linearly polarized signals are demultiplexed by a series of FSSs, which have large oblique angles with respect to the direction of propagation. In this particular case, the incidence angles are 27.5° for FSS#1, and 45° for FSS#2 and FSS#3. A proposed quasi-optical multiplexer frequency separation scheme and the optical layout for the FY-4 microwave radiometer are shown in Figs. 1(b) and 1(c), and the transmission and reflection ray paths of the quasi-optical beams are also shown. Firstly, the beam coming from the reflector is separated by polarization filter P. Only partial waves with 54-GHz and 380-GHz horizontal polarization signal are transmitted, while vertical polarization signals at 118, 183, and 425 GHz are reflected. Then three frequency selective surfaces are used to separate different channels: FSS#1 separates 54-GHz and 380-GHz beams; FSS#2 and FSS#3 separate 118-GHz, 183-GHz, and 425-GHz beams.

Table 1. Electrical requirements for the five-frequency-band multiplexer.

Frequency band	Polarization	Insertion losses	15-dB half-beam bandwidth	Cross polarization
54±4 GHz	H or V			
118.75±6 GHz	H or V			
183.310±8 GHz	H or V	< 0.8 dB	4.3°±0.1°	< −22 dB
380.197±19.5 GHz	H or V			
424.763±5 GHz	H or V			

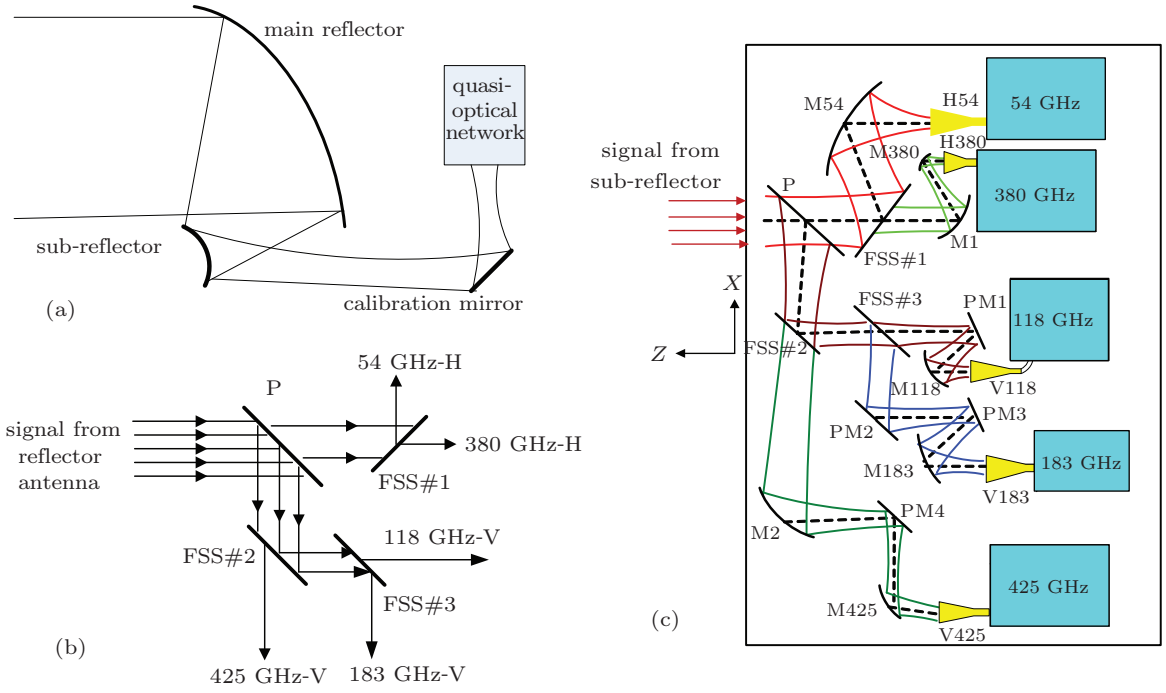


Fig. 1. (colour online) Schematic of the quasi-optical system. (a) Whole structure of the microwave payload. (b) Quasi-optical multiplexer frequency separation scheme. (c) Quasi-optical multiplexer optics layout.

2. Design of the FSS filter

In the quasi-optical feed chain network, the quasi-optical FSS filter design is critical. The design of the structure is particularly challenging. Due to the tight spatial electrical constraints and the weak signal from Earth or space, it requires low-loss splitting of the incident beam over a large range of incidence angles. Furthermore, the FSS is required to provide very high isolation between two adjacent frequency bands in order to distinguish different molecular spectral signals. The work described in this paper is motivated by the need to provide a technical solution to facilitate the detection and analysis of radiation for weather forecasting and climate research which are planned by FY-4. The design objective is to design three quasi-optical filters which separate the five frequency bands with an insertion loss of less than 0.4 dB and separation between adjacent channels of more than 20 dB. The electromagnetic performance of the three FSS filters are summarized in Table 2.

Table 2. The electromagnetic performance of the three FSS filters. The $w_{\rm t}$ and $w_{\rm r}$ denote the transmission band and reflection band, respectively, δ is the transmission insertion loss, σ is the separation between transmission and reflection band, and $\theta_{\rm i}$ is the incident angle.

	$w_{\rm t}$/GHz	$w_{\rm r}$/GHz	δ/dB	σ/dB	$\theta_{\rm i}$	Polarization model
FSS#1	360–400	50–58	< 0.4	> 20	27.5	TE
FSS#2	419—429	112–125, 175–192	< 0.4	> 20	45	TM
FSS#3	112–125	175–192	< 0.4	> 20	45	TM

FSS#1 separates the frequency bands 50–58 GHz and 360–400 GHz with insertion loss less than 0.4 dB and separation between channels more than 20 dB in the TE plane at incidence angle of 27.5°. FSS#2 filter is designed to allow transmission of 419–429 GHz with a loss less than 0.4 dB and reflection of 175–192 GHz and 112–125 GHz with separation between channels more than 20 dB at incidence angle of 45° in the TM plane. FSS#3 has the ability to separate the frequency bands of 175–192 GHz and 112–125 GHz with insertion loss less than 0.4 dB and separation between channels in excess of 20 dB in the TM plane at an incidence angle of 45°.

In the millimeter and sub-millimeter wave bands, two types of FSS are commonly used, which are the waveguide-array FSS and the printed FSS.[2−7] The waveguide-array FSS filter consists of one or several metal plates containing an array of closely-spaced apertures arranged on an arbitrary lattice. According to waveguide theory, it reflects the signal below the cutoff frequency of the fundamental mode and transmits the higher-frequency signal. There are several design parameters which determine the electromagnetic performance of the waveguide-array FSS: (i) the structural dimensions of the waveguide apertures, (ii) the center-to-center spacing of the apertures, and (iii) the plate thickness. The printed FSS filter consists of arrays of conductive elements on or between the dielectric substrates. It shows band pass or band stop characteristics, which offers considerable flexibility in the design. The frequency bandwidths are largely determined by the element type and size, the lattice geometry, and the electrical properties of the substrate. Sharper roll-off of the spectral response curve can be achieved by cascading two or more closely-spaced arrays.[8] FSS filters used in millimeter and sub-millimeter wave bands are usually constructed by printing arrays of self-resonant periodic metal elements on the surface of thin SiO_2 wafers,[9,10] because this material is suitable for use in space and has a low-loss tangent, and the electrical design parameters in the millimeter and sub-millimeter wave bands can found in manuals.[11] However, the above-mentioned structures also have many disadvantages. In detail, for the waveguide-array FSS filter, the angular sensitivity is relatively low, insertion loss is high, narrow bandwidth for large incidence angle, and only high pass filter can be designed which limits the application flexibility. For the multilayer printed FSS, the loss is dependent on the frequency separation between transmission and reflection bands. Hence, when it is required to cascade several FSS to achieve a sharp roll off, the insertion loss is often unacceptable. The propagation of electromagnetic waves through a multilayer structure has acted as a Fairy–Perot interferometer from the physical optics standpoint.[12] The total length of the path becomes much longer as a result of multiple reflections between layers, so the loss becomes significant. Moreover, structural robustness must be taken into consideration when using this type

of FSS. Since in very high working frequencies, like millimeter and sub-millimeter waves, the substrate would be very thin, it is likely to be damaged due to the typical launch forces found in space applications.

To overcome these disadvantages at millimeter and sub-millimeter wavelengths, a new type of freestanding FSS has been developed, which uses thin self-supporting air-spaced screens aligned with a proper resonant unit. It has superior spectral performance and structural robustness. Since it has no substrate, the insertion loss due to dielectric absorption is removed.[13] Therefore, it is able to improve the power signal-to-noise ratio of the quasi-optical system. In order to meet the insertion loss requirement and specified spectral transmission response, we adopt this structure. The most important step in the design of FSS is the proper choice of resonant element. We choose the short–ring slot unit due to its simplicity in manufacturing. By connecting the ring slot elements and adjusting the length of the ring slot, the frequency response can be designed to resonate at desired center frequency for either TM or TE polarization.[14] A shorted C-shaped ring slot element is adopted in this study, as shown in Fig. 2. According to the polarization direction of the incident electric field with respect to the direction of the shorted junction, the new type of resonant unit is able to excite equivalent even-mode and odd-mode magnetic currents. When the incident electric field is parallel to the shorted junction (TM incidence), the shorted ring slot unit has dual resonance, the lower resonant frequency is half of the resonant frequency of the ring slot unit ($\lambda_0/2$ mode, λ_0 is the vacuum wavelength corresponding to the resonant frequency of the ring slot unit), and the higher frequency is 1.5 times of the resonant frequency. Conversely, when the incident electric field is perpendicular to the shorted junction (TE incidence), the resonant frequency is very close to that of the ring slot. To achieve higher packing density, a unit cell consisting of a shorted ring slot which resonates at the $\lambda_0/2$ mode is used. The benefit is that it makes the element period smaller, resulting in a compact structure. This configuration is able to widen the transmission bandwidth and inhibit the generation of grating lobes. However, the pass band characteristic of the single-layer FSS is too narrow to satisfy the low insertion loss requirement, and the transmission roll-off above resonance is too weak to provide the required separation between adjacent channels. The spectral response performance can be improved by cascading two aligned identical screens . Meanwhile, the FSS array elements behave similarly to conventional periodic arrays, and the element spacing avoiding the grating lobes should obey the same rule that governs a conventional array antenna.[15] A triangular lattice arrangement with a 60° skew grid is used to attain a broader pass-band characteristic, due to the increase in packing density which is obtained through geometrical arrangement. Finally, we design three freestanding FSS filters, one of which is defined as a periodic structure without supporting materials in the proximity of the resonant unit. Mechanical integrity is provided by a proper thick dielectric annulus located outside of the active region of the filter. Each FSS filter consists of shorted ring slot units by designing the elements to resonate at the required center frequency of interesting bands. It is able to provide the transmission response in agreement with the required performance specification. The geometry of the FSS structure with two aligned air spaced metal screens is shown in Fig. 3. The T_x and T_y are the periodic

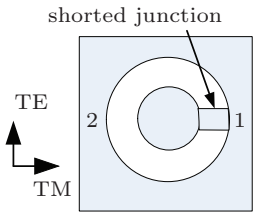


Fig. 2. (colour online) Schematic of the shorted ring slot resonant unit.

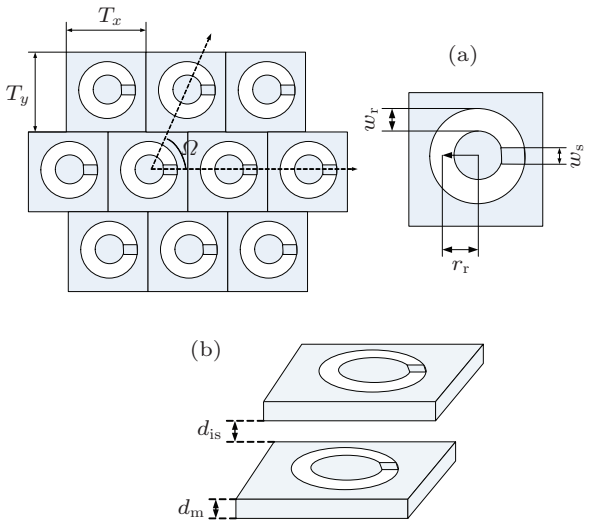


Fig. 3. (a) Top view of the FSS filter structure. Left: the periodic arrangement structure; right: the structural dimensional parameter of the resonant unit including r_r, w_r, and w_s. (b) Side view: two aligned air-spaced screens.

spacings in the x and y directions, respectively, and $\Omega = 60°$ is the skew grid angle. The resonant element has three structural parameters: the radius ($r_{\rm r}$) and width ($w_{\rm r}$) of the resonant unit, and the width ($w_{\rm s}$) of the shorted junction, which are able to be optimized to achieve the required specification. The "$d_{\rm is}$" is the interlayer separation, and $d_{\rm ms}$ is the thickness of the metal screen.

To predict the characteristics of the FSS filter, the computer simulation technology (CST) Microwave Studio is used to optimize the FSS design and obtain the physical dimensions of the structure. The CST can model the thickness of the slots and the effect of the finite surface conductivity of the metal. In the computer models, the metal thickness $d_{\rm m}$ is 0.0125 mm and metal copper is used. By applying appropriate excitation and boundary conditions, the response of the periodic array can be analyzed using a single 3D unit cell. The optimizing structural parameters of the three FSS filters are summarized in Table 3.

Table 3. Structural parameters (in units of mm) for the three FSS filters.

	$T_x(T_y)$	$r_{\rm r}$	$w_{\rm r}$	$w_{\rm s}$	$d_{\rm is}$
FSS#1	0.4	0.16	0.05	0.05	1
FSS#2	0.3	0.075	0.1	0.05	0.2
FSS#3	0.7	0.25	0.15	0.2	0.7

3. Simulation performance and discussion

The simulation results of FSS#1, FSS#2, and FSS#3 are shown in Figs. 4–6. Figure 4 shows the predicted results of FSS#1 orientated at the incidence angle of 27.5° for a linearly polarized TE signal. The calculated loss in the transmission band varies between 0.11 and 0.22 dB at 360 GHz and 400 GHz, respectively. The maximum loss over the designated range of frequencies is smaller than 0.25 dB. Similarly, the reflection loss is less than 0.02 dB. The FSS#2 yields about 0.26-dB insertion loss in the band of 419–429 GHz, and 25-dB isolation in the bands of 112–125 GHz and 175-192 GHz. Computed transmission coefficients are plotted in Fig. 5. It is shown that the insertion loss of the polarized TM FSS at resonance (425 GHz) is 0.24 dB, and exhibits loss in the range 0.22–0.26 dB in pass band. Figure 6 shows that the insertion loss is 0.13 dB at resonant (118 GHz) for FSS#3, the maximum insertion loss is 0.2 dB at lower edge of the lower sideband (112 GHz) for TM polarization, and the insertion loss varies between 0.13 and 0.2 dB. The transmission and reflection results are summarized in Table 4.

Table 4. Calculated results of co-polarization reflection and transmission for the three FSS filters.

Frequency/GHz	Reflection/dB			Transmission/dB		
	FSS#1	FSS#2	FSS#3	FSS#1	FSS#2	FSS#3
50	–0.01	–	–	–46.02	–	–
54	–0.01	–	–	–45.04	–	–
58	–0.02	–	–	–44.03	–	–
112	–	–0.017	–18.61	–	–33.33	–0.2
118	–	–0.017	–26.8	–	–32.75	–0.13
125	–	–0.018	–26.04	–	–32.09	–0.14
175	–	–0.027	–0.05	–	–27.77	–24.89
183	–	–0.029	–0.03	–	–27.08	–29.05
192	–	–0.032	–0.03	–	–26.30	–34.15
360	–22.98	–	–	–0.15	–	–
380	–15.52	–	–	–0.22	–	–
400	–26.35	–	–	–0.11	–	–
419	–	–31.01	–	–	–0.22	–
425	–	–43.77	–	–	–0.23	–
429	–	–29.84	–	–	–0.25	–

From the above tables, it is concluded that the maximum reflection loss is 0.02 dB at 58 GHz for FSS#1 in the TE plane. Such values at the lower edge of the two lower frequency bands are 0.0018 dB (125 GHz) and 0.032 dB (192 GHz) for FSS#2, and 0.05 dB (175 GHz) for FSS#3 in the TM plane.

From the above-mentioned results, it is concluded that the maximum loss in the transmission and reflection losses is below 0.4 dB in either TE or TM plane. These FSS filters exhibit a maximum insertion loss of 0.25 dB, more than 20 dB rejections for either TE or TM polarization. Therefore, these FSS filters satisfy our requirements in the frequency range of interest, and even exceed the requirement performance specifications.

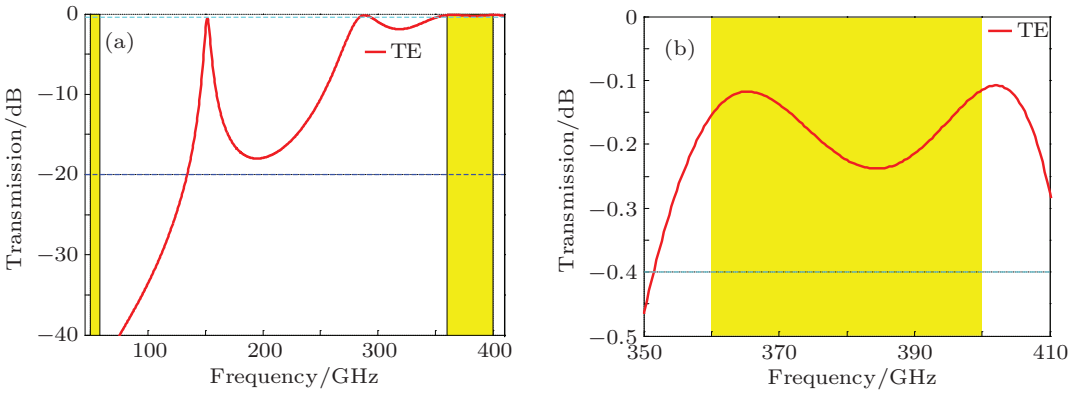


Fig. 4. (colour online) (a) Predicted transmission responses of FSS #1 with two air-spaced aligned screens orientated at the incidence angle of 27.5° in the TE plane. (b) Enlarged view of the resonant transmission peaks.

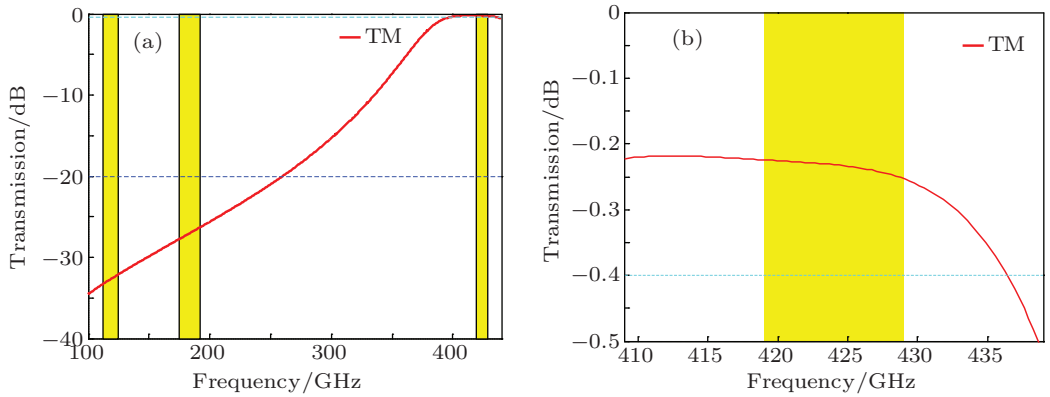


Fig. 5. (colour online) (a) Predicted transmission responses of FSS #2 with two air-spaced aligned screens orientated at the incidence angle of 45° in the TM plane. (b) Enlarged view of the resonant transmission peaks.

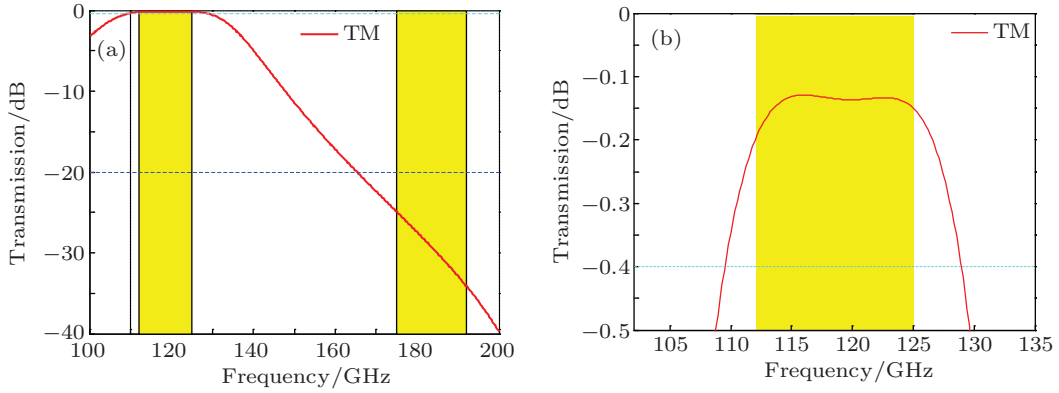


Fig. 6. (colour online) (a) Predicted transmission responses of FSS #3 with two air-spaced aligned screens orientated at the incidence angle of 45° in the TM plane. (b) Enlarged view of the resonant transmission peaks.

In practical application, the feed antenna illuminating the FSS filter has a finite beam width, and therefore it does not irradiate an ideal uniform plane wave but a bunch of paraxial Gaussian beams. According to the Fourier optics, it contains many angular spectrum components considered to be a group of plane waves traveling with different amplitudes at different angles.[16] Thus, these plane waves will not all reach the FSS filter at the same angles, as shown in Fig. 7. Therefore, the electrical performance of the FSS filter must be optimized for a range of incidence angles, typically a boundary angle of ±5°. The frequency responses of additional boundary angles are shown in Figs. 8–10.

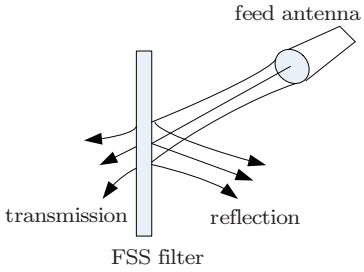


Fig. 7. Schematic of transmission and reflection when the feed antenna illuminates the FSS filter.

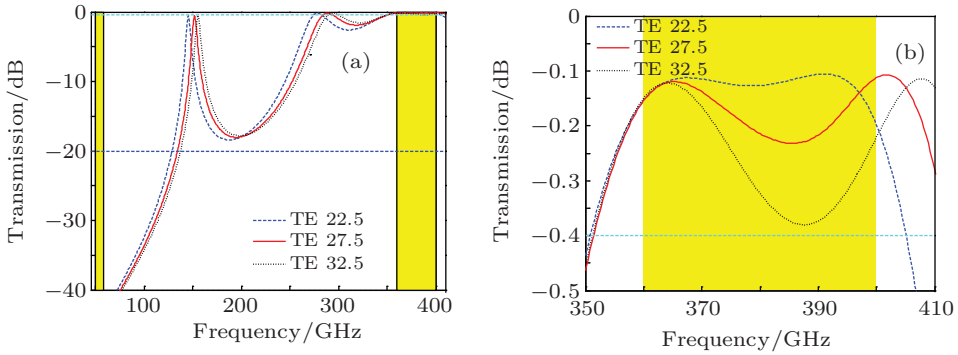


Fig. 8. (colour online) (a) Frequency response curve of the FSS#1 with respect to the angle variation. (b) An enlarged view.

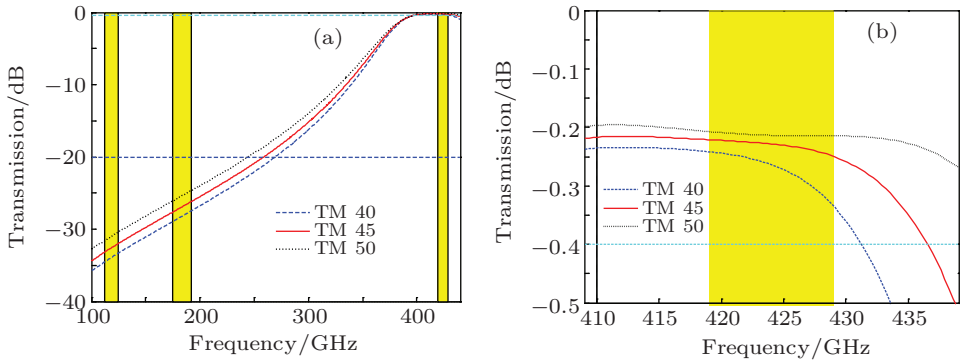


Fig. 9. (colour online) (a) Frequency response curve of the FSS#2 with respect to the angle variation. (b) An enlarged view.

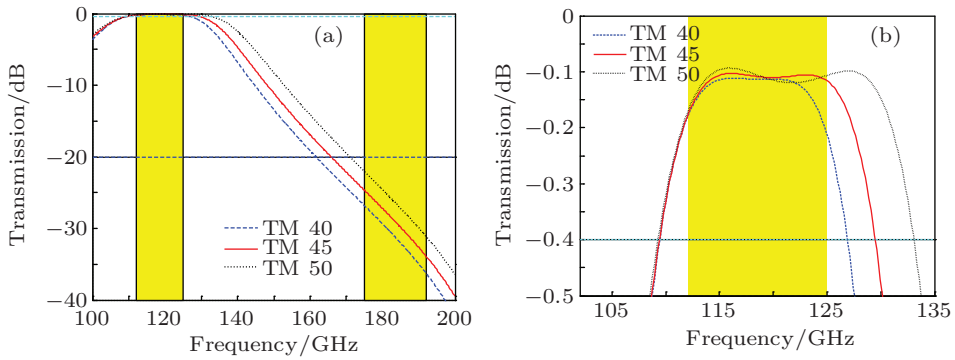


Fig. 10. (colour online) (a) Frequency response curve of the FSS#3 with respect to the angle variation. (b) An enlarged view.

The FSS#1 filter exhibits a noticeable performance change at incidence angles of 22.5°, 27.5°, and 32.5°, but it is always better than 0.4 dB in the pass band. The performance changes of the FSS#2 and FSS#3 filters are trivial at incidence angles of 40°, 45°, and 50°. It is confirmed that the type of filter is less sensitive to the angle variation within a certain angle range from the above results. The frequency response of the three filters is able to meet the system performance requirement, with not only the nominal angle of incidence but also different angles within a certain range taken into consideration.

Finally, a parameter sensitivity study was conducted to determine the fabrication tolerances based on a maximum acceptable insertion loss increase of 0.1 dB. The fabrication tolerances of FSS#1, FSS#2, and FSS#3 are listed in Table 5.

Table 5. Fabrication tolerances of the three FSS filters.

Structural parameter	Fabrication tolerance/μm		
	FSS#1	FSS#2	FSS#3
$T_x(T_y)$	±8	±6	±10
$r_{\rm r}$	±4	±4	±5
$w_{\rm r}$	±7	±10	±11
$w_{\rm s}$	±5	±5	±18
$d_{\rm is}$	±76	±31	±71

Fabrication tolerances of ±4 μm for the $r_{\rm r}$, $w_{\rm r}$, $w_{\rm s}$, and periodicity (T_x or T_y), and ±31 μmfor the interlayer separation ($d_{\rm is}$) are found to satisfy the criteria that the performance degradation is below 0.1 dB. The preferred manufacturing method is compatible with that of the existing mature integrated circuit (IC) and micro-electro-mechanical system (MEMS) fabrication process, of which fabrication tolerances within ±2 μm can be obtained.

4. Conclusion

A freestanding FSS structure used in millimeter and sub-millimeter wavelengths is reported, and the designs of three FSS filters intended for application in FY-4 are described in this paper. We have designed three FSS filters to demultiplex linearly polarized energy in the frequency range of 50–429 GHz with a maximum target loss of 0.4 dB for large incidence angles up to 27.5° or 45°. These three FSS filters are used to filter either TE or TM polarized signal. Numerical simulations using software CST is carried out. The simulation results show that the maximum transmission insertion loss is 0.25 dB, and the reflection loss is 0.05 dB in the specified bands. The separation between adjacent channels is greater than 25 dB. These FSS filters satisfy the requirements that the insertion loss is less than 0.4 dB and image rejection is greater than 20 dB. They even exceed the requirement performance specifications. It is concluded that the insertion loss of this novel FSS filter structure is significantly lower than that of the FSS printed on dielectric. It is suitable for application at millimeter and sub-millimeter wave bands. The fabrication of such an FSS is compatible to the present mature IC process, and the fabrication error is easy to control at a micron level.

References

[1] Martin R J and Martin D H 1996 *Electron Comm.* **18** 37

[2] Cahill R and Parker E A 1980 *Electron. Lett.* **16** 710

[3] Parker E A 1981 *IEE Proc Microw Opt. Antennas* **3** 17

[4] Cahill R and Parker E A 1982 *Electron. Lett.* **18** 313

[5] Hamdy S M A and Parker E A 1982 *Electron. Lett.* **18** 624

[6] Zhuang W, Chen R S, Ding D Z and Wang D X 2009 *Microw. Opt. Tech. Lett.* **11** 2567

[7] Lu J, Wang J B and Sun G C 2009 *Chin. Phys.* B **18** 041598

[8] Munk B A 2000 Frequency *Selective Surfaces: Theory and Design* (New York: Wiley)

[9] Dckie R Cahill R and Fuso V F 2004 *IEE Proc. Microw. Antennas Propag.* 31

[10] Cahill R and Gamble H S *24th ESTEC Antenna Workshop on Innovative Periodic Antennas: Photonic Band Gap Fractal and Frequency Selective Surfaces* (Holland: European Space Agency) p. 103

[11] Cahill R and Parker E A *Electron. Lett.* **31** 1752

[12] Lima A C and Parker E A 1996 *Proc. IET Microw. Antennas Propag.* **143** 157

[13] Dicke R and Cahill R 2005 *Proc. IEEE Antennas Propag.* **53** 1903

[14] Churpin A D Parker E A and Batchelor J C 2000 *Electron Lett.* **36** 1601

[15] Lo Y T and Lee S W 1988 *Antenna Handbook* (New York: Reinhold Co.) pp. 13.13-13.20

[16] Chen J C 1994 *TDA Progress Report* JPL p. 42